Articles

Photochemically Induced Nuclear Polarization Study of the Accessibility of Tyrosines in Insulin†

Karol A. Muszkat,* Igor Khait, and Shulamit Weinstein

ABSTRACT: The accessible tyrosines of bovine insulin were studied by the photochemically induced dynamic nuclear polarization (photo-CIDNP) method. Tyrosine ^{1}H nuclear polarization is observed in acidic, neutral, and basic solutions at all concentrations studied, in the absence of added salts as well as in the presence of 0.05–0.1 M chloride or phosphate. At pH 2.1 in the presence of chloride, at concentrations of 640 μM and above, most of the nuclear polarization at δ 6.82 originates from one group of tyrosines. On the basis of the crystallographic model, these are assumed to be the A14 tyrosines. We explored the possibility of a genuine concentration dependence of the photo-CIDNP intensity of insulin due to aggregation. In order to discern between such effects and trivial kinetic effects traceable to the optical irradiation method, the effects of concentration changes on polarization were examined in three apparently nonassociating trypsin inhibitor proteins. In insulin, the intensity of Tyr-A14 polarization changes slowly at concentrations above 1 mM, suggesting that these residues are similarly accessible in all association states. At insulin concentrations below 320 μM, additional tyrosine emission signals were observed. These signals are probably due to B16 and B26 tyrosines of monomers. Polarization transfer effects from Tyr-A14 are evident in the tetramer and hexamer. Enhanced absorption effects in the two histidines (B5 and B10) of the insulin monomer were observed at pH 10 in the presence of 0.1 M phosphate.

Tyrosine residues play important roles in the hydrophobic interactions of insulin, such as those involved in the different aggregation stages of this hormone and in its binding to the specific receptors on cell membranes [see, e.g., Blundell et al. (1972, 1971), Dodson et al. (1979), Feng et al. (1980), Insulin Research Group (1974), Piron et al. (1980), Goldman & Carpenter (1974), and Pocker & Biswas (1980)]. These are the interactions which control and regulate the transport and storage as well as the reactivity of this hormone.

Of the four tyrosines of most mammalian insulins, three (A19, B16, and B26) are species invariant and seem to form part of a larger receptor binding (and activity-determining) surface, which also includes residues Gly-A1, Gln-A5, Asn-A21, Val-B12, Phe-B24, and Phe-B25 (Feng et al., 1980; Piron et al., 1980).

Aggregation to dimer and hexamer, similar in many respects to receptor binding, involves close contacts of tyrosines at the two interunit interfaces, along the OP and OQ local axes of the hexamer [cf. Blundell et al. (1972)], as can be deduced from the crystal structure of the two Zn hexamer of bovine insulin. The formation of the "crystal" dimer in solution involves close contact of monomers along the OP local hexamer axis (Blundell et al., 1972). The tyrosines taking part are Tyr-B16 from one monomer subunit which interacts with Gly-B′8, Ser-B′9, and Val-B′12 from the other subunit, and Tyr-B26 which interacts with Tyr-B′16, Gly-B′23, and Phe-B′24 (the prime denoting residues of the second monomer). Likewise, in the building up of hexamers from dimers (along the local OQ axis), Tyr-A14 interacts with Tyr-A′14 and with Phe-B′1, both from the other dimer unit.

Apart from equilibrium constants at low concentrations (Jeffrey & Coates, 1966a,b; Goldman & Carpenter, 1974), no experimental data are available on the rates and paths of the processes interconnecting the principal aggregation states of insulin—monomer, dimer, tetramer, and hexamer (denoted subsequently as I_1, I_2, I_4, and I_6). Because of difficulties traceable to aggregation and to low solubility, only a few detailed results could be obtained thus far by studying insulin in water solutions by conventional nuclear magnetic resonance spectroscopy [see, e.g., Bradbury et al. (1981) and references cited therein, Bradbury & Brown (1977), and Williamson & Williams (1979)]. In particular, these studies provided only limited information on the important tyrosine residues, especially in neutral solutions.

Significant progress in the study of tyrosine (and other) residues in single or interacting proteins, in solution, under physiological conditions has been made possible recently by the very specific photochemically induced dynamic nuclear polarization (photo-CIDNP) method [see, e.g., Muszkat (1977), Muszkat & Gilon (1977, 1978), Muszkat et al. (1978, 1982, 1983), Berliner & Kaptein (1981) and references cited therein, and Lerman & Cohn (1980)]. The CIDNP effects (reffered to also as nuclear polarization) consist of changes in intensity and sign of the normal, equilibrium NMR transitions of nuclei of molecules originating from the components of a transient, electron-spin-correlated, radical pair. In proteins, the transient radical pair is obtained by a chemically reversible hydrogen atom abstraction process by a dye molecule photoexcited to its triplet state [see, e.g., Muszkat & Weinstein (1975, 1976)].

Compared to NMR, and even more so, compared to other spectral methods, photo-CIDNP offers several important advantages for the study of proteins and of their interactions.

The foremost is that of chemical specificity. Thus, e.g., only the nuclei of the particular tyrosine residue undergoing hydrogen transfer show nuclear polarization. In this sense, CIDNP provides a true (though ephemeral) nuclear spin-label for those molecules which take part in the H atom transfer cycle. This factor is important in the common situation of

† From the Departments of Structural Chemistry (K.A.M. and I.K.) and Organic Chemistry (S.W.), The Weizmann Institute of Science, Rehovot 76100, Israel. *Received March 2, 1983.* Supported in part by the U.S.–Israel Binational Science Foundation, Jerusalem, Israel.

0006-2960/84/0423-0005$01.50/0

overlapping NMR signals encountered in the aromatic proton region.

Another significant advantage of CIDNP is that of the inherent signal amplification. Typical enhancements, on the order of 5–15, are very common in proteins, though much larger effects have been observed in small peptides (Muszkat, 1977; Muszkat & Gilon, 1977, 1978; Muszkat et al., 1978).

Finally, hydrogen atom transfer in tyrosine requires true contact of abstractor and donor molecules at the relative atoms, which is only possible for exposed residues. Thus, polarization is diagnostic of significant accessibility of tyrosine residues to the photoexcited dye probe. A similar conclusion holds for histidine polarization, while tryptophan polarization, due largely to reversible electron transfer, is probably less exigent as it could also take place at some distance.

At an early stage in the development of the photo-CIDNP method of protein study, we investigated bovine insulin in solution (9.7 mM in ^2H_2O) at pH 2.4 (Muszkat et al., 1978). We observed strong nuclear polarization in the well-resolved H-3 and H-5 aromatic doublet of a single tyrosine, a result which necessarily indicates considerable accessibility of this tyrosine (see below) to the photoexcited dye molecule.

Following the recent availability of a much more refined experimental technique [e.g., see Muszkat et al. (1982, 1983)], we have reexamined the insulin system under a wide range of conditions in an attempt to detect possible tyrosine accessibility changes originating not only from different states of aggregation but also from possible differences in conformations of the insulin unit in the monomer and in the dimer, tetramer, and hexamer. However, to appreciate fully the magnitude of the problem, we have to note that in the absence of any degeneracy, an aggregation pattern, as in insulin (monomer, asymmetric dimer, tetramer, and hexamer), can lead to eight enumerable (different) residues originating from each monomer residue.

Materials and Methods

Bovine crystalline zinc insulin (Sigma Chemical Co., St. Louis, MO, catalog no. I-5500, actual zinc content 0.46%) was used throughout. Fresh solutions in ^2H_2O (>99.7 atom % ^2H) were used. These were prepared by dissolving in ^2H_2O in the presence of a minimum amount of ca. 1 M ^2HCl and adjusting the pH to the desired value with ca. 1 M NaO^2H solution. To obtain equilibrium, the solutions were left at room temperature for 1 h before measurements. Concentrations of insulin are given in terms of the monomer unit, assuming complete dissociation. Most measurements were carried out at 25 °C. Urea-d_4 (>98 atom % ^2H) was obtained from the Aldrich Chemical Co., Milwaukee, WI. As accessibility probe (dye), we used 10-(carboxyethyl)flavin at a 3×10^{-4} M concentration. It was kindly provided by Dr. D. Porter, Department of Biochemistry and Biophysics, University of Pennsylvania, Philadelphia, PA. The proton 270-MHz photo-CIDNP and dark spectra were measured on a Bruker WH270 NMR spectrometer. In earlier experiments, the spectrometer was operated by a BNC-80 computer with the FTQUAD-80 program, but all later measurements were carried out with the Aspect-2000 computer and FTQNMR program. The photo-CIDNP spectra were measured by a modified Fourier method as described previously [see, e.g., Muszkat & Gilon (1978) and Muszkat et al. (1982)]. Every optical irradiation (0.3–0.4-s duration) is preceded by a 15-s cooling delay and followed by a magnetic relaxation delay (D_3) 0.05 s or longer. The radio-frequency pulse and free induction decay (FID) data acquisition follow, in the usual way. At low insulin concentrations, the accumulation of 40–100 FID acquisitions was required. The light source used is a 5000-W mercury–xenon lamp operated at 3500 W. The light beam is collimated by a quartz lens system and filtered through a 23-cm-thick water layer to remove the infrared component. The concentration-dependence experiments (see below) were repeated by using a filter composed of a 15-cm-thick water layer and an 8-cm-thick 5% $CuSO_4$ layer, transmitting in the 330–550-nm region. Following 90° reflection and focusing, light is admitted to the sample region by a quartz light guide. The light guide is rigidly connected to the sample tube (Muszkat et al., 1982).[1] The operation of the whole setup is controlled by the spectrometer's computer. As the chemical shift and intensity standard, we used (4–6) $\times 10^{-4}$ M 4,4-dimethyl-4-silapentane-1-sulfonate (DSS). We define an apparent polarization P' as

$$P' = \Delta I / I_D = \Delta I / (I_L - \Delta I) \quad (1)$$

where I_D is the dark spectrum intensity, I_L is the signal intensity in the light spectrum, and ΔI is the signal intensity in the light minus dark difference spectrum. The absolute polarization P is defined as

$$P = \Delta I / I_s \quad (2)$$

where I_s is the intensity of a standard signal, usually DSS. P is thus a direct measure of the number of polarized molecules. The sample of bovine pancreatic trypsin inhibitor (BPTI, Trasylol) used was provided by the Bayer AG, Werk Bielefeld, FRG. Pure samples of the Kunitz soybean trypsin inhibitor [STI; see, e.g., Ikenaka et al. (1974)] and of the chickpea inhibitor [CI; see, e.g., Belew & Eaker (1976)] were provided by Dr. M. Vered, Department of Agricultural Biochemistry, Faculty of Agriculture, The Hebrew University, Rehovot, Israel.

Table I: Weight Distribution of Insulin among Aggregation States at pH 2.0 in 0.05 M NaCl[a]

	[I] (μM)						
	80	160	310	620	1240	2480[b]	4960[c]
I_1	0.50	0.40	0.31	0.23	0.16	0.10	0.01
I_2	0.47	0.53	0.58	0.57	0.51	0.36	0.12
I_4	0.03	0.07	0.10	0.17	0.25	0.38	0.57
I_6			0.01	0.03	0.08	0.16	0.30
P^d	0.12	0.25	0.4	1.3	2.17	2.64	3.4

[a] Data are taken from Jeffrey & Coates (1966a,b). Abbreviations: I_1, insulin monomer; I_2, insulin dimer; I_4, insulin tetramer; I_6, insulin hexamer. [b] Extrapolated values. [c] Approximate values. [d] Absolute polarization (eq 1) of the signal at δ 6.82 measured in terms of the DSS signal at δ 0, in the presence of 0.05 M NaCl and 5.5×10^{-4} M DSS at pH 2.1.

Results and Discussion

The following systems were investigated, mostly at 25 °C. The complexity data listed in Table I of Blundell et al. (1972) were assumed. (a) The first was insulin (I), up to 4960 μM, at pH 2.1 in the presence of 0.05 M NaCl. The aggregate distribution (weight fraction) in this system at concentrations up to 2300 μM was studied by Jeffrey & Coates (1966a,b).

[1] The light intensity at the exit of the collector lenses is ca. 40 W. Only a small fraction of this intensity is transmitted to the coil region. The most severe loss occurs in the light guide. In our setup, it transmits only 7% of the incident light. No significant amount of UV light below 365 nm reaches the coil region. An optical irradiation period of 0.3–0.4 s is required for obtaining a maximum effect, the same as required when using a 1.3-W 488-nm argon ion laser in the "through coil" optical configuration.

Table II: Distribution of A14 Tyrosines among Interdimer (A) and Monomer (M) States at Different Concentrations of Insulin at pH 2

	[I] (μM)													
	80		160		310		620		1240		2480		4960	
	M	A	M	A	M	A	M	A	M	A	M	A	M	A
I_1	0.50		0.40		0.31		0.23		0.16		0.10		0.01	
I_2	0.46		0.53		0.58		0.57		0.51		0.36		0.12	
I_4	0.03	0.02	0.035	0.035	0.05	0.05	0.085	0.085	0.125	0.125	0.19	0.19	0.285	0.285
I_6						0.01		0.03		0.08		0.16		0.30
	0.98[a]	0.02[a]	0.965[a]	0.035[a]	0.94[a]	0.06[a]	0.885[a]	0.115[a]	0.795[a]	0.205[a]	0.65[a]	0.35[a]	0.415[a]	0.585[a]

[a] Total values.

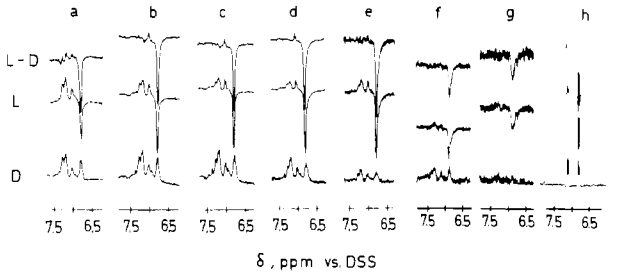

FIGURE 1: Aromatic proton region of the 270-MHz proton photo-CIDNP spectra of bovine insulin in ^2H_2O, in the presence of 3×10^{-4} M 10-(carboxyethyl)flavin. DSS (5.5×10^{-4} M) is used as the δ 0 chemical shift standard. (D) Dark spectra; (L) light spectra; (L − D) light minus dark difference spectra. In (a–g), the pH is 2.1, and the concentration of NaCl is 0.05 M. Insulin concentrations, expressed as the micromolar concentration of monomer, were (a) 4960, (b) 2480, (c) 1240, (d) 620, (e) 310, (f) 160, and (g) 80 μM; (h) *N*-acetyltyrosine, 2×10^{-3} M. In (b–d) and (f), the intensity of D is twice the intensity of L and L − D. In (h), the intensity of D is 4 times that of L and L − D. Complexity data are given in Table I.

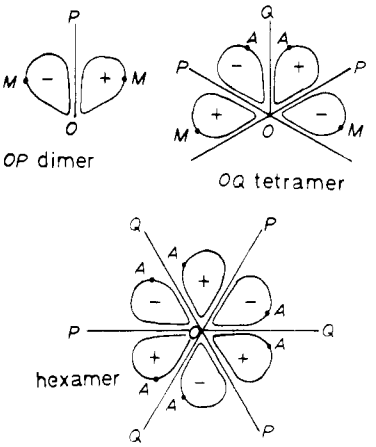

FIGURE 2: Schematic representation of the assumed structure of natural (solution) dimer, tetramer, and hexamer [after Blundell et al. (1972)]. A and M represent interdimer and monomer Tyr-A14 residues, respectively (see text).

These weight fractions, extrapolated up to 2480 and 4960 μM, are given in Table I. Over this concentration range, the monomer weight fraction decreases from 0.50 at 80 μM to 0.10 at 2480 μM. The change in the dimer fraction is small, ca. 25% (e.g., 0.46 at 80 μM and 0.36 at 2480 μM). The weight fraction of tetramer increases, from 0.04 at 80 μM to 0.38 at 2480 μM, while the hexamer is perceptible only at 310 μM, ca. 0.01, increasing to 0.16 at 2480 μM. Some experiments were carried out at 4960 μM, where the tetramer and hexamer are the main species. (b) The second was a 1740 μM solution at pH 2.3 and 57 °C. Under these conditions, significant dissociation to monomer takes place. (c) The third was 1300 μM insulin in the presence of 8 M urea-d_4 at pH 7.1, in ^2H_2O. This system also undergoes significant dissociation to monomer. (d) The fourth was 950 μM insulin at pH 6.8 and 9.0. Under these conditions, the hexamer predominates. (e) The fifth was 640 μM solution at pH 3.5. (f) The sixth was the same as (e), but in the presence of excess zinc ion. The aromatic proton region spectra of the light and dark spectra measured under these conditions are given in Figures 1 and 3–6.

System a. These measurements (Figure 1a–g) were carried out at several insulin concentrations in the range of 80–4960 μM. Part of this range, up to 2300 μM, is covered in the molecular weight distribution study of Jeffrey & Coates (1966a,b) (see Table I). As in earlier measurements at 9.7 mM insulin concentration and 90 MHz (Muszkat et al., 1978), the strongly negative tyrosine 3,5-proton signal shows one well-resolved doublet (Figure 1a–f). The width of this doublet is comparable with that of a single free tyrosine (Figure 1h). The resolved components in Figure 1a–d should thus be attributed to one type of tyrosine common to all or most aggregation forms. The light signals are narrower than the merged dark signals at δ 6.8, indicating that of all tyrosines contributing to the dark δ 6.8 signal only one group gives rise to the narrow CIDNP signal (cf., e.g., Figure 3B with Figure 1d, spectrum L–D). On the basis of the crystallographic model of the two Zn insulin hexamer (Blundell et al., 1972), the resolved polarized signals should be assigned to the A14 tyrosine, which are clearly the most accessible. Obviously, such an assignment should be valid provided the crystal conformation of the hexamer and of its units is retained in all aggregation forms in solution.

It is possible to divide the A14 tyrosines into two subsets, e.g., "monomer" residues (M), as in monomer and dimer, and interdimer residues (A), as shown in Figure 2. The calculated distribution of these two states at various insulin concentrations is given in Table II. The absolute polarization values (listed in Table I) for the millimolar range of concentration do not indicate significant differences in the accessibility of the two subsets A and M (see Appendix).

The present observation may be variously affected by several chemical processes of the type

$$I_i + I_j \rightleftharpoons I_k + I_l \rightleftharpoons I_m + I_n \qquad (3)$$

As the all-important data on the rates (and even paths) of the processes interconnecting the four major aggregation states are unavailable, it is difficult at present to obtain a clear picture on the factors responsible for these results. Nevertheless, the fact that over the wide range of concentrations and of system compositions we obseve one well-resolved Tyr-A14 signal common to dimer, tetramer, and hexamer (see Figure 1a–f) may have several implications. One such implication could be that all 3 and 5 aromatic Tyr-A14 protons are highly degenerate or, less likely, that the interconnecting processes are fast on the NMR time scale ($>10^7$ s^{-1}). Another implication of which we should be aware is that for the above reason

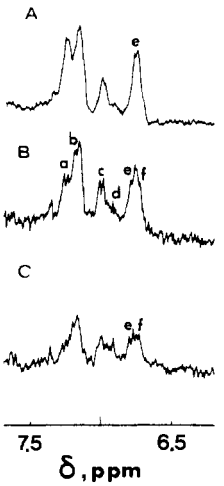

FIGURE 3: 270-MHz ^1H NMR spectra of insulin solutions at pH 2.1 in the presence of 0.05 M NaCl. (A) 4960 μM insulin; (B) 620 μM insulin; (C) 160 μM insulin.

we are unable to discern between degenerate nuclear polarization distribution processes such as the indirect process

$$I_k \xrightarrow{\text{photo-CIDNP}} I_k^*$$

followed by

$$I_k^* + I_l \rightarrow I_n^* \quad (4)$$

and the direct process

$$I_n \xrightarrow{\text{photo-CIDNP}} I_n^* \quad (5)$$

An indirect process such as 4 could gain importance if the rate of the reaction $I_k + I_l \rightarrow I_n$ is not slower than the rate of relaxation of nuclear polarization (on the order of 1 s; see, e.g., Figure 5 and 6). It is interesting to note that in a related situation of molecular association in several proteinase (A)–protein inhibitor (B) complexes (Muszkat et al., 1982, 1983), it is possible to rule out the possibility of creation of polarization in the AB complex by an indirect process, e.g.

$$A^* + B \rightarrow A^*B$$

or

$$A + B^* \rightarrow AB^*$$

At concentrations of 310 μM and below, the tyrosine emission signal broadens as other tyrosine emission signals appear at δ 6.72 and δ 6.65. Their relative weight increases with decreasing concentration. The width of these signals should be compared with that of a completely accessible tyrosine, shown in Figure 1h.

In the absence of further information, and on the basis of the crystallographic model, we suggest the assignment of the signals at δ 6.72 and δ 6.65 to Tyr-B16 and -B26, respectively, of the natural (solution) monomer. In the dimer, as well as in the higher association forms, these two tyrosines would be buried and thus inaccessible to the probe dye. However, both are at least partially accessible in the monomer if that part of the molecule retains its two Zn hexamer crystal structure [see, e.g., Figure 5b of Blundell et al. (1972)]. Another possibility to consider is that the δ 6.72 signal is due to Tyr-A14 of the monomer. The positive signals in the L–D curves of Figure 1b–d should probably be assigned to the 2,6 ring protons of the Tyr-A14. The normal dark spectra of the aromatic protons of insulin (Figure 3) also show pronounced concentration effects (e.g., signals a, c, and f), some of which largely parallel those observed in the photo-CIDNP spectra

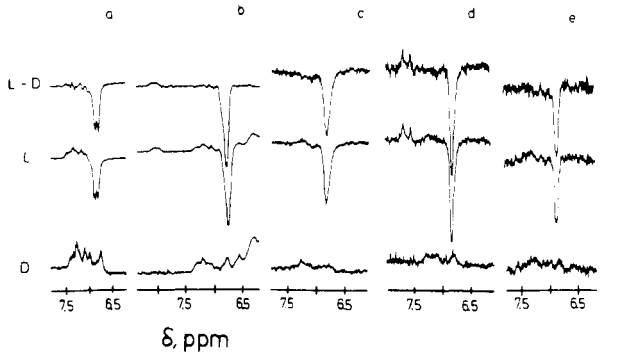

FIGURE 4: Photo-CIDNP spectra of the aromatic region of insulin (cf. the caption to Figure 1). (a) 1740 μM insulin at pH 2.3 and 57 °C; (b) 1300 μM insulin in the presence of 8 M urea-d_4 at pH 7.1; (c) 950 μM insulin at pH 6.8; (d) 870 μM insulin at pH 10.0 in the presence of 0.1 M Na_2HPO_4 (enhanced signals at δ 7.58 and δ 7.72 are due to C-2 protons of histidines-B5 and -B10); (e) 640 μM insulin at pH 3.5 in the presence of 1.1 mM $ZnSO_4$. In (b) and probably in (a), the main molecular species is the monomer while in (c) and (e) it is the hexamer.

of Figure 1. Thus, going from 4960 to 320 μM reveals a new tyrosine 3,5-proton doublet (f in Figure 3C), in addition to the Tyr-A14 doublet e in Figure 3A. Such a signal indicates that the light signal at δ 6.72 corresponding to f in Figure 1 originates from a principal component of the system.

The accessibility of Tyr-A19 is believed to be only little affected by association-state changes. Inferring from its position in the two Zn hexamer crystal, it seems probable that it is inaccessible to the 10-(carboxyethyl)flavin probe in all association states of insulin.

System b: A 1740 μM Solution at pH 2.3 and 57 °C. Compared with CIDNP spectra measured at similar total concentrations, at 25 °C (e.g., Figure 1b,c), the CIDNP spectrum at 57 °C (Figure 4a) shows a new tyrosine signal at δ 6.7. Thus, in analogy with the system of Figure 1e–g, this new signal is assigned to tyrosines-B16 and -B26 of the monomer, and furthermore, we conclude that under these conditions the monomer accounts for a significant fraction of all complexity species.

System c: 1300 μM Insulin in the Presence of 8 M Urea-d_4 at pH 7.1. The tyrosine emission signal (Figure 4b) is significantly broadened compared with its width shown in Figure 1c. We attribute this effect to the accessibility of all tyrosines because of complete dissociation of all higher complexity forms and because of significant loss of helix structure, as a result of breaking of internal hydrogen bonds. It is thus not unexpected to observe here an unresolved positive signal at δ 8.1 we attribute to the protons of otherwise inaccessible histidines (B5 and B10). While inaccessible in the hexamer, these histidines are accessible in the lower complexity species. However, at an acidic pH, these histidines are unobservable because of protonation of the imidazolyl ring.

System d: 870 μM Insulin at pH 10 in the Presence of 0.1 M Na_2HPO_4. The monomer is the predominating species under these conditions. Enhanced absorption signals of the C-2 imidazolyl protons of His-B5 and -B10 are apparent at δ 7.58 and δ 7.72 (see Figure 4d). At this pH value, the tyrosine signal at δ 6.8 is narrower than that at, e.g., pH 2.1 (Figure 1g), probably due to different conformations of the monomer at pH 2.1 and pH 10.

System e: 950 μM Insulin at pH 6.8 and 350 μM Insulin at pH 7.1 in the Presence of 0.1 M Phosphate. The hexamer is the main species under these conditions. Again, the tyrosine emission signal (Figure 4c and Figure 6b) is attributed mainly to Tyr-A14. The significant width of this signal when com-

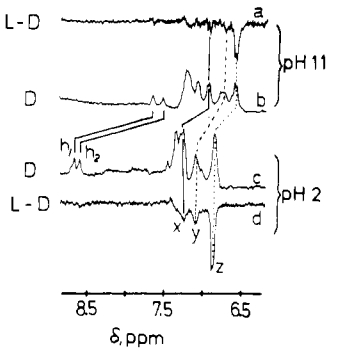

FIGURE 5: Correlation and probable assignment of aromatic proton signals of insulin at pH 2 and 11. (D) Dark spectra; (L − D) cross-relaxation-modified photo-CIDNP spectra. The cross-relaxation delay was 0.3 s. Assignments: y, doublet, 2 and 6 Tyr-A14 protons; z, 3 and 5 Tyr-A14 protons; h_1 and h_2, C-2 protons of histidines-B5 and -B10. Concentrations are 6.9 mM in (a) and (b) and 6.3 mM in (c) and (d).

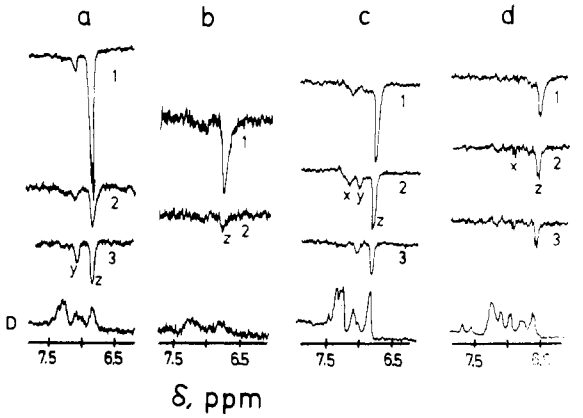

FIGURE 6: Polarization transfer (cross-relaxation) effects on aromatic protons in CIDNP spectra of bovine insulin solutions in ^2H_2O in the presence of 3×10^{-4} M 10-(carboxyethyl)flavin. (D) Dark spectra; (1–3) cross-relaxation-modified photo-CIDNP (L − D) spectra. The cross-relaxation delay was 0.05 s in (1), 0.3 s in (2), and 0.5 s in (3). (a) 650 μM insulin at pH 3.5; (b) 350 μM insulin at pH 7.1, in the presence of 0.1 M phosphate; (c) 6.3 mM insulin at pH 2 in the presence of 0.05 M NaCl; (d) 6.9 mM insulin at pH 11. For the assignment of signals x and z, see the legend to Figure 5 and the text. Note the polarization transfer effects on signals x and y. Tetramer and hexamer are major complexity forms.

pared to that of Figure 1a at pH 2.1 is possibly the result of restricted rotation about the ring–methylene single bond at the higher pH. Indeed, the polarization relaxation rate at pH 7.1 (Figure 6b) is much faster than those at pH 2 and 3.5 (spectra a and c, respectively, of Figure 6).

System f: A 650 μM Solution at pH 3.5 in 1.1 mM $ZnSO_4$. The tyrosine signal in the spectrum of Figure 4e, in the presence of a 2-fold excess of zinc, is not significantly broadened compared to its width in the absence of a large zinc excess (signal at δ 6.8, Figure 6a).

Significant nuclear polarization transfer effects were observed in insulin solutions under a variety of conditions [for a recent discussion of such effects in the lactalbumin series, see Berliner & Kaptein (1981) and references cited therein]. Such effects are shown in Figure 6a,c as well as in Figure 5, curve d. The emission signals at δ 7.3 and δ 7.15 denoted respectively as x and y in Figure 5d and Figure 6a,c are due to polarization transfer, as an increase in the postoptical irradiation delay (D_3) from 0.05 (curve 1 in Figure 6a,c) to 0.3 and 0.5 s (curves 2 and 3, respectively) results in the growing in of these signals. Even when D_3 is kept short (e.g., 0.05 s) as in spectrum 1 of Figure 6a, considerable polarization builds up in the receiving nuclei y at δ 7.15. This growing in is due

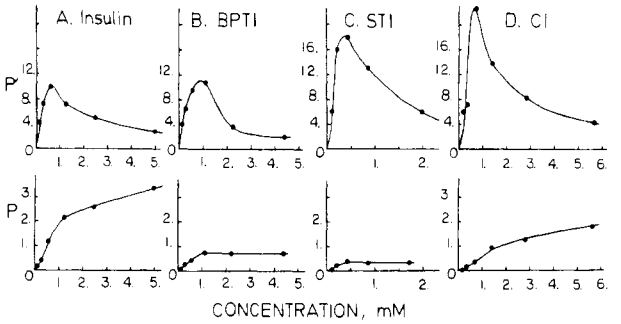

FIGURE 7: Dependence of the apparent polarization (P') and the absolute polarization (P) (eq 3 and 4) on the concentration in insulin and in three reference proteins. (A) Insulin (M_r 5750), pH 2.1, 0.05 M NaCl, δ 6.82; (B) BPTI (M_r 6500), pH 7.2, δ 7.3; (C) STI (M_r 21 500), pH 7.4, δ 6.53; (D) CI (M_r 8000), pH 2.1, 0.05 M NaCl, δ 6.77. The reference compound was 5.5×10^{-4} M DSS, δ 0.

to the finite length of the optical irradiation, 0.4 s, which allows the buildup of primary polarization in the z protons and its subsequent transfer to the δ 7.15 and δ 7.3 nuclei (y and x, respectively). Prolonging the D_3 delay to 0.3 and 0.5 s, as in curves 2 and 3 of Figure 6 results in the growth of the secondary polarization at δ 7.15 and in the decay of the primary polarization. The intensity ratio for y/z varies from 0.12 at D_3 = 0.05 s to 0.5 at D_3 = 0.5 s, while the secondary polarization in the x signal passes through a maximum at D_3 = 0.3 s.

Signals x and y in Figure 6a,c should probably be identified with signals b and c of Figure 3B and thus are both 2,6 ring tyrosine protons. However, while y and seems to be identifiable with Tyr-A14, the exact assignment of x to a definite tyrosine is yet unestablished. One possible correlation between aromatic region spectra at pH 2 at 6 mM (main species: tetramer and hexamer) and pH 11 is given in Figure 5.

Appendix

Analysis of Protein Photo-CIDNP Intensity Effects. The possibility of detecting changes of accessibility of tyrosines (in particular, Tyr-A14) in the four aggregation states of insulin was examined by studying the concentration dependence of the intensity of the polarized signals in a constant light intensity and constant dye concentration (optical path) regimen. Thus, comparing[2] the concentration-dependence pattern with that determined for a nonassociating protein should permit us to detect, at least in principle, accessibility changes in the same residue in the different aggregation states. Under the present optical irradiation conditions at constant dye concentration and constant light intensity (light intensity limited conditions), the range of protein concentrations going from 10^{-4} to 10^{-2} M covers two different regions. In the trivial concentration-dependence region (a), at the lowest protein concentrations, only part of the triplet dye molecules formed are intercepted by protein molecules. The apparent and absolute polarization intensities, P' and P, respectively (eq 1 and 2), are small and increase rapidly with increasing protein concentration until a maximum value of P' and a constant (or slowly increasing) value of P are reached (see Figure 7), corresponding to the second concentration region (b). In the plateau region of P (b), all triplet dye molecules are intercepted by the protein. A further increase of protein concentration lowers the apparent polarization P' due to dilution of polarized with inert substrate molecules. The absolute polarization remains unaffected (Figure 7B,C) or rises slowly (Figure 7D) over this range. The

[2] We are indebted to a referee for suggesting this comparison.

results with the three reference proteins BPTI, STI, and CI [for previous photo-CIDNP results, see, e.g., Muszkat et al. (1983)] indicate that region b is reached at 0.4 mM in STI (at pH 7.4), at 0.8 mM in BPTI (at pH 7.2), and at 0.8 mM in CI (at pH 2.1 and in 0.05 M NaCl), while in CI no plateau of P seems to be reached up to 5.6 mM. The decrease in P' in the trivial dependence region (a) is roughly comparable for all proteins studied.

The concentration dependence of the polarization, P, in insulin reported in Table I seems to be qualitatively comparable with the results obtained for the three reference proteins (see Figure 7). Thus, insulin shows the same polarization decrease over the trivial dependence region (a), at concentrations below 0.8 mM. Over region b, above 0.8 mM, the observed polarization increase is small, comparable to that observed for CI. Therefore, no evidence is available at present to indicate accessibility differences between the tyrosines of the different association states of insulin. For equal molar concentrations, the absolute polarization obtained for insulin is significantly higher than that of the reference proteins.

Registry No. Tyr, 60-18-4; insulin, 9004-10-8.

References

Belew, M., & Eaker, D. (1976) *Eur. J. Biochem. 62*, 499–508.

Berliner, L. J., & Kaptein, R. (1981) *Biochemistry 20*, 799–807.

Blundell, T. E., Dodson, G. G., Dodson, E., Hodgkin, D. C., & Vijayan, M. (1971) *Recent Prog. Horm. Res. 27*, 1–40.

Blundell, T., Dodson, G., Hodgkin, D., & Marcola, D. (1972) *Adv. Protein Chem. 26*, 279–401.

Bradbury, J. H., & Brown, L. R. (1977) *Biochemistry 16*, 573–582.

Bradbury, J. H., & Ramesh, V. (1981) *J. Mol. Biol. 150*, 609–613.

Dodson, E. J., Dodson, G. G., Hodgkin, D. C., & Reynolds, C. D. (1979) *Can. J. Biochem. 57*, 469–479.

Feng, Y. M., Gu, J. L., Zhang, X. T., Lu, Z. X., Xu, W. J., & Zhu, J. H. (1980) *Insulin, Chemistry, Structure and Function of Insulin and Related Hormones* (Brandenburg, D., & Wollmer, A., Eds.) pp 455–460, de Gruyter, West Berlin.

Goldman, J., & Carpenter, F. H. (1974) *Biochemistry 13*, 4566–4574.

Ikenaka, T., Odani, S., & Koide, T. (1974) *Bayer-Symp. 5*, 325–343.

Insulin Research Group (1974) *Sci. Sin. (Engl. Ed.) 17*, 779–792.

Jeffrey, P. D., & Coates, J. H. (1966a) *Biochemistry 5*, 489–498.

Jeffrey, P. D., & Coates, J. H. (1966b) *Biochemistry 5*, 3820–3824.

Lerman, C. L., & Cohn, M. (1980) *Biochem. Biophys. Res. Commun. 97*, 121–125.

Muszkat, K. A. (1977) *J. Chem. Soc., Chem. Commun.*, 872–873.

Muszkat, K. A., & Weinstein, M. (1975) *J. Chem. Soc., Chem. Commun. 34*, 143–144.

Muszkat, K. A., & Weinstein, M. (1976) *Z. Phys. Chem. (Wiesbaden) 101*, 105–114.

Muszkat, K. A., & Gilon, C. (1977) *Biochem. Biophys. Res. Commun. 79*, 1059–1064.

Muszkat, K. A., & Gilon, C. (1978) *Nature (London) 271*, 685–686.

Muszkat, K. A., Weinstein, M., & Gilon, C. (1978) *Biochem. J. 173*, 993–996.

Muszkat, K. A., Weinstein, S., Khait, I., & Vered, M. (1982) *Biochemistry 21*, 3775–3579.

Muszkat, K. A., Weinstein, S., Khait, I., & Vered, M. (1983) *Biopolymers 22*, 387–390.

Piron, M. A., Michiels-Place, M., Waelbroeck, M., De Meyts, P., Schuttler, A., & Brandenburg, D. (1980) *Insulin, Chemistry, Structure and Function of Insulin and Related Hormones* (Brandenburg, D., & Wollmer, A., Eds.) pp 371–391, de Gruyter, West Berlin.

Pocker, Y., & Biswas, S. B. (1980) *Biochemistry 19*, 5043–5049.

Williamson, K. L., & Williams, R. J. P. (1979) *Biochemistry 18*, 5966–5972.